Timescales of Magmatic Processes and Eruption Ages of the Nyiragongo volcanics from ^{238}U-^{230}Th-^{226}Ra-^{210}Pb disequilibria.

Ramananda Chakrabarti [1#*], Kenneth W. W. Sims[2, 3], Asish R. Basu[1], Mark Reagan[4], Jacques Durieux[5]

1. Department of Earth and Environmental Sciences, University of Rochester, Rochester, NY-14627

2. Department of Geology and Geophysics, Woods Hole Oceanographic Institution, Woods Hole, Massachusetts, MA 02543

3. Dept of Geology and Geophysics, University of Wyoming, Laramie, WY 82071

4. Department of Geoscience, University of Iowa, Iowa City, Iowa 52242

5. Deceased, formerly at Unite De Gestion Des Risques Volcaniques, UNDP / UNOPS, Goma - Nord-Kivu - RD Congo

Current address: Department of Earth and Planetary Sciences, Harvard University, Cambridge, MA 02138

* Corresponding author - email: rama@eps.harvard.edu

Keywords: Silica-undersaturated volcanism, ^{238}U-^{230}Th-^{226}Ra-^{210}Pb series disequilibria, Magma transport and residence time, Carbonate metasomatism, Volcanic hazard assessment.

Abstract

The silica-undersaturated Nyiragongo volcanics, located in the East African rift, have globally unique chemical compositions and unusually low viscosities, only higher than carbonatite lavas, for terrestrial silicate magmas. We report ^{238}U-^{230}Th-^{226}Ra-^{210}Pb series disequilibria in 13 recent and prehistoric lava samples from Nyiragongo including those from the 2002 flank eruption and a 2003 lava lake sample. ($^{230}Th/^{238}U$) ranges from 0.90-0.97 in the recent lavas and from 0.94-1.09 in the prehistoric lavas. To explain the variable ^{230}Th and ^{238}U excesses in these lavas, we hypothesize that different processes with opposite effects in terms of fractionating Th/U in the mantle source are involved. These processes include: 1) low degree partial melting of a phlogopite-bearing mantle source (consistent with low K/Rb) with residual garnet (consistent with high chondrite-normalized Dy/Yb), to produce the observed ^{230}Th excesses; and, 2) carbonate metasomatism for the ^{238}U enrichment, consistent with high Zr/Hf in the Nyiragongo lavas.

The Nyiragongo volcanics have higher ($^{230}Th/^{232}Th$) values than observed in most mantle-derived rocks, especially ocean-island basalts, suggesting that their mantle-source was affected by carbonate metasomatism less than 300 ka ago. Several Nyiragongo samples display significant ^{226}Ra excesses implying rapid magma transport (less than 8 ka) from the mantle-source to the surface. Modeling the observed ($^{226}Ra/^{230}Th$) versus Zr/Hf correlation in the lavas indicates that the 2002, 2003 and a few pre-historic lavas incorporated 50-60% of a carbonate-metasomatized mantle source while the other pre-historic lavas show 10-22% contribution of this source. This result indicates that the Nyiragongo lavas were derived from a heterogeneous, non-uniformly carbonated mantle source. The 2002 lava shows ($^{210}Pb/^{226}Ra$) equilibrium, whereas the 2003 lava lake sample

shows initial ($^{210}Pb/^{226}Ra$) < 1. The latter observation suggests that Nyiragongo magmas degas as they rise to the surface over years or decades before eruption. ($^{210}Pb/^{226}Ra$) equilibrium in the 2002 lava suggests that the 2002 magma may have stagnated for more than a decade before eruption. The high CO_2 content, high emission rates, extreme fluidity, along with the inferred short residence time and our inferences of rapid magma transport and high eruptive frequency suggest that the volcanic hazards of Nyiragongo, both from lava flows and gas emissions, are higher than previously estimated.

1. Introduction

Volcanism in the East African Rift System (Fig. 1) includes acid, intermediate, mafic alkalic and ultrabasic magmatism with contrasting compositions between the volcanics to the north and the south (Baker et al., 1971; Furman, 2007). The relatively more voluminous volcanism to the north is related to the Afar deep-mantle plume with flood basalt eruptions commencing ~30 Ma ago in northern Ethiopia and Yemen (Schilling et al., 1992; Pik et al., 1999). Towards the south the East African Rift splits into two halves, the Kenyan rift in the east and the western rift to the west of Lake Victoria. Volcanism in the southern part and the associated topographic uplift (Kenyan dome) are thought to be surface manifestations of another mantle plume (Pik et al., 2006).

The Virunga Volcanic Province (VVP), located in the western rift (Fig. 1), is characterized by unusual silica-undersaturated, ultra-alkaline mafic volcanism that started ~11 Ma ago and has continued to present. Of the two currently active volcanoes of the VVP, Nyiragongo and Nyamuragira (Fig. 1), Nyiragongo is compositionally unique and has received considerable attention for its unusual mineralogy and petrology (Holmes and Harwood, 1937; Sahama and Smith, 1957; Sahama, 1960; Sahama, 1973; Demant et al., 1994; Platz et al., 2004; Chakrabarti et al., 2009). There is isotopic and geochemical evidence indicating that these volcanics were derived from a heterogeneous mantle plume (Chakrabarti et al., 2009).

Nyiragongo was the focus of global attention in January 2002 as the erupted lava, with extremely low viscosity, rapidly overran the city of Goma causing a significant humanitarian crisis (Baxter et al., 2002-2003; Komorowski et al., 2002 - 2003; Tedesco et al., 2007). Thermal and rheological properties of this lava (Giordano et al., 2007) suggest

the dry viscosities of the Nyiragongo lava to be among the lowest measured in terrestrial magmas with only carbonatites having even lower viscosities (Dawson et al., 1990). Despite the significance of Nyiragongo in the global spectrum of volcanic activity and lava composition, there are very few constraints on either its eruptive history or the magmatic processes generating its compositionally distinct lavas.

In this study, we have analyzed ^{238}U-^{230}Th-^{226}Ra-^{210}Pb disequilibria in 13 lava samples (Fig. 1) from the Nyiragongo volcano, including 4 historic lava samples from 2002 and 2003 and 9 unknown-age samples. The vastly different half-lives and variable chemical properties of these ^{238}U-decay series nuclides enable us to use these measurements to: 1) determine eruption age limits for the prehistoric lavas, and, 2) evaluate the processes and timescales of the magmatic processes generating these extremely silica-undersaturated mafic lavas. Determining eruption ages is critical for hazard assessment in that these ages could provide constraints on Nyiragongo's resurfacing rate and eruptive cyclicity.

2. Samples of the present study

13 Nyiragongo lava samples were analyzed. These include multiple 2002 flow samples, a 2003 lava lake sample and several prehistoric, unknown age samples from parasitic cones and plugs on the volcanoes flanks. The locations of the Nyiragongo samples are shown in Figure 1 and tabulated in Table 1. The Nyiragongo lavas are typically aphyric to microcrystalline, showing a porphyritic texture with small phenocrysts of melilite, kalsilite, leucite, Ti-augite, and olivine in a fine-grained glassy groundmass. Petrographically discernible groundmass minerals, as observed in the pre-historic lava

samples, include kalsilite, nepheline and smaller amounts of leucite with minor clinopyroxene, olivine, perovskite, apatite, calcite and titanomagnetite (Sahama, 1973) although calcite was not identified in any of the representative recent and prehistoric lava samples from a wider sample set (Chakrabarti et al., 2009), which include some of the lava samples analyzed in the present study. The lavas of Nyiragongo are unique both compositionally and in their physical properties and to the best of our knowledge are unmatched by any other terrestrial occurrence. These lavas are strongly alkaline and silica-undersaturated and show high concentrations of compatible and incompatible trace elements including light rare earth elements (LREE) and high field strength elements (HFSE) (Chakrabarti et al., 2009). Based on normative mineralogy, these lavas are classified as melilitite, melilite nephelinite, pyroxene nephelinite, leucitite, and leucite nephelinite (Platz et al., 2004). These extreme normative compositions of the Nyiragongo lavas differ significantly from other volcanoes of the VVP, (e.g. Rogers et al., 1998) including Nyamuragira (e.g. Aoki et al., 1985; Chakrabarti et al., 2009), which is located only 15 km to the north of Nyiragongo (Fig. 1b).

3. Methods and Results

Approximately 12 grams of 1–5 mm sized rock chips were carefully hand-picked and then ultrasonicated in sequential batches of 18 M ohm H_2O, 2% high purity H_2O_2 and 0.1M Seastar HCl for 5 minutes in each step, before being crushed. Note that such mild leaching, as has been shown in experiments using subaerial rock standards (e.g. TML and AThO), does not perturb the U/Th, Th/Ra and U/Pa of the samples (Sims et al., 1999; 2002; Bourdon et al., 2000). In addition, as discussed below, the overall consistency of our mass

129 spectrometry data on leached samples and alpha spectrometry data on unleached aliquots of
130 the same samples further indicates that mild leaching has not fractionated U, Th, Pb and Ra
131 in our samples.

132 U, Th and Ra concentrations (using isotope dilution) and isotopic ratios were
133 determined using the Thermo Fisher Element 2 (sector field ICPMS) and Neptune (MC-
134 ICPMS) at the Woods Hole Oceanographic Institution (WHOI) (Ball et al., 2008; Sims et
135 al., 2008a; Sims et al., 2008b). Activity of ^{226}Ra was also determined using gamma
136 spectrometry at WHOI (Appendix Table 1) while ^{210}Pb activity was determined by
137 measurement of ^{210}Po using alpha spectrometry at the University of Iowa. Details of the
138 analytical methods are given in Appendix 1 and in Sims et al. (2008a, b) and Reagan et al.
139 (2005). U and Th concentrations of the lava samples of the present study and activity ratios
140 of ^{238}U/^{232}Th, ^{230}Th/^{232}Th, ^{230}Th/^{238}U, ^{226}Ra/^{230}Th and ^{210}Pb/^{226}Ra (selected samples) are
141 shown in Table 2 along with those of USGS rock standards BCR-2 (Columbia River
142 basalt), ATHO (Icelandic obsidian) and TML (Table Mountain latite) processed and
143 analyzed together with the Nyiragongo samples. For completeness ^{87}Sr/^{86}Sr, Zr/Hf, and
144 chondrite-normalized (Sun and McDonough, 1989) Dy/Yb of the Nyiragongo samples are
145 also tabulated in Table 2 (See Chakrabarti et al. (2009) for a complete tabulation of major
146 and trace element concentrations and Sr, Nd and Pb isotopic abundances of these samples).
147

148 *3.1. (^{238}U/^{232}Th), (^{230}Th/^{232}Th), and (^{230}Th/^{238}U)*

149 Th/U ratios (Table 2) of the Nyiragongo volcanics range from 2.16 to 2.33 for the
150 2002 and 2003 lavas and from 2.31 to 3.00 for the older lavas. (^{238}U/^{232}Th) for the
151 Nyiragongo volcanics range from 1.01 to 1.41 while (^{230}Th/^{232}Th) ranges from 1.04 to 1.36.

The youngest lava samples from Nyiragongo (2002 and 2003) show varying excesses in ^{238}U. These samples plot to the right of the equiline in Figure 2 and the activity ratio ($^{230}Th/^{238}U$) for these four samples range from 0.90 to 0.97. ($^{230}Th/^{238}U$) for the older Nyiragongo volcanics range from 0.94 to 1.09 and these samples plot on both sides of the equiline although the offsets are not large (Fig. 2). Internal errors are much less than 1% (2σ) for ($^{230}Th/^{232}Th$). However, when propagated uncertainties related to tail correction are included, the errors are ~ 1% for ($^{230}Th/^{232}Th$). The errors for ^{238}U and ^{232}Th concentration determinations are ~0.5-1% based on both internal precision and uncertainties in spike calibration and propagated errors for ($^{238}U/^{232}Th$) are 1-2 %. For some samples (e.g. NY-37a) the external reproducibility on separate powder dissolutions is ~ 4% for ($^{230}Th/^{238}U$), which is higher than the internal precision and uncertainties in spike calibration suggesting that the sample powders are slightly heterogeneous. USGS standards, BCR-2, ATHO and TML analyzed in this study yield ($^{230}Th/^{238}U$) of 1.00, 1.10 and 1.00, respectively, which are in agreement with the expected values for these standards (Table 2) (Sims et al., 2008a). Our results are in good agreement with earlier alpha-spectrometry analyses of U-Th disequilibria for Nyiragongo lavas (Vanlerberghe et al., 1987; Williams and Gill, 1992) but are in sharp contrast to the recent findings of Tedesco et al. (2007) who reported ($^{238}U/^{232}Th$) activity ratios ranging from 1.48 to 2.81 and ($^{230}Th/^{232}Th$) ranging from 0.99 to 1.40 for 2002 and 2003 Nyiragongo lavas which translate to ($^{230}Th/^{238}U$) activity ratios significantly less than unity (0.43-0.85) and are outside of the disequilibria yet measured in any samples in the global U-Th data base (see Sims and Hart, 2006 for global compilation). Their ($^{230}Th/^{232}Th$) are similar to our study and previous findings (Vanlerberghe et al., 1987; Williams and Gill, 1992), but their

175 ($^{238}U/^{232}Th$) is considerably different. We believe that the differences in the ($^{230}Th/^{238}U$)
176 data of Tedesco et al. (2007) and other data (this study; Vanlerberghe et al., 1987; Williams
177 and Gill, 1992) arise mainly from differences in Th concentration measurements. While our
178 data were obtained by high-precision isotope dilution mass spectrometry, the data reported
179 in Tedesco et al. (2007) were obtained by unspiked alpha spectrometry.
180
181 *3.2. ^{210}Pb-^{226}Ra-^{230}Th*
182 ($^{226}Ra/^{230}Th$) measured by MC-ICPMS range from 1.06 to 1.12 for the 2002 and
183 2003 lavas of Nyiragongo, and from 1.00 to 1.12 for the older unknown age Nyiragongo
184 lava samples. Of the 13 Nyirangongo samples measured for ($^{226}Ra/^{230}Th$), seven (including
185 the 2002 lava flow samples and the 2003 lava lake sample) have ($^{226}Ra/^{230}Th$) significantly
186 greater than unity. For Ra measurements, internal precision is 1-2 % similar to the
187 uncertainties in the ^{228}Ra spike calibration and the NIST ^{226}Ra standard against which the
188 spike was calibrated.
189 Activities of selected short-lived isotopes for most of the samples of the present study
190 were also determined by gamma-counting at WHOI (See Sims et al., 2008a for details).
191 These activities are shown in Appendix Table 1. Activity of ^{226}Ra was determined by proxy
192 measurements of ^{214}Pb (using the 351.99 keV energy line) and ^{214}Bi (using the 609.32 keV
193 energy line). All activities are reported in disintegrations per minute per gram (dpm/gm).
194 As shown in Appendix Table 1, the activity of ^{226}Ra obtained from mass spectrometry and
195 the gamma counting are consistent within analytical uncertainties. The magnitude of Ra-Th
196 disequilibria determined in this study (Table 2) is significantly different from those of
197 Tedesco et al. (2007) who have reported ($^{226}Ra/^{230}Th$) ranging from 1.27 to 1.89 for the

198 Nyiragongo lavas from the 2002 eruption and the 2003 lava lake sample. Although the
199 (^{226}Ra) data of Tedesco et al. (2007) are similar to our data, the difference in the measured
200 (^{226}Ra/^{230}Th) is a result of the significantly different Th concentrations determined in that
201 study by unspiked alpha spectrometry.

202 ^{210}Pb ($t_{1/2}$ ~22.6 years) was determined for one 2002 lava (NY-1-02) and the 2003
203 lava lake sample of Nyiragongo by analyzing its daughter nuclide ^{210}Po between April and
204 September, 2008. (Table 2). Replicate ^{210}Po activities for the whole-rock 2003 lava lake
205 sample were 6.38 and 6.54 dpm/g (both ± 0.22, 2σ). The average (^{210}Po) for triplicate
206 analyses of the NY-1-02 whole rock was 7.45 +/- 0.32 (2σ) dpm/g (Table 2). This value
207 and all three individual measurements for NY-1-02 were within analytical error of the
208 (^{226}Ra) value for the whole rock 2002 indicating a ^{210}Pb/^{226}Ra activity ratio of unity. In
209 contrast, the initial (^{210}Pb /^{226}Ra) values for the 2003 lava lake sample calculated from the
210 replicate (^{210}Po) measurements were 0.90 and 0.92.

211

212 **4. Discussion**

213 *4.1. Age constraints of the Nyiragongo lavas with implications for volcanic hazard*
214 *assessment for the city of Goma and vicinity:*

215 The Nyiragongo volcanics are unique in the global spectrum of volcanism because of
216 their unusual compositions, low viscosities and high effusion rates. In addition, this
217 volcano is located only 15 km to the north of the city of Goma, with a population of over
218 500,000 (Fig. 1). Given the high fluidity of the Nyiragongo lavas (Giordano et al., 2007)
219 and the presence of a persistent lava lake (Tazieff, 1995) this volcano presents a significant
220 threat to the inhabitants of Goma, which is located on a fracture zone. Lavas from the 2002

eruption of Nyiragongo engulfed parts of the city of Goma in a matter of few hours upon eruption killing 170 people and displacing over 350,000 inhabitants (Baxter et al., 2002-2003; Komorowski et al., 2002 - 2003; Tedesco et al., 2007). The only other documented historical eruption of Nyiragongo in 1977 resulted in a humanitarian crisis of similar proportions (Durieux, 2002-2003). There are several other lava flows of Nyiragongo whose ages are not constrained. Hence, it is not clear how often this volcano erupts. Determining Nyiragongo's eruption history is important for understanding its resurfacing rate and eruptive cyclicity.

Common methods for dating Quaternary age volcanics using $^{40}Ar/^{39}Ar$ dating and surface exposure dating with cosmogenic nuclides cannot be reasonably applied to most of the Nyiragongo lavas because of their very young eruption ages and the rapid reforestation and surface erosion rates in this region. U- and Th- decay series nuclides have a wide range of half-lives (seconds to 75,000 years) and chemical properties and can thus be used to date basalts as young as ~0.05 years to 350,000 years (e.g. Rubin and Macdougall, 1990; Goldstein et al., 1991; Goldstein et al., 1994; Rubin et al., 1994; Sims et al., 1995, 2003, 2007, 2008b). The observation that all the Nyiragongo lavas analyzed in this study show significant ^{238}U-^{230}Th disequilibria limits the eruption ages of the prehistoric Nyiragongo samples to less than 300 ka.

Three samples from the 2002 lava flow, the 2003 lava lake sample and three other relatively older (unknown age) samples show ($^{226}Ra/^{230}Th$) significantly greater than unity (Table 2). For these unknown age lavas the ^{226}Ra excesses limit the eruption ages of the lavas to less than 8 ka. Five other prehistoric lava samples from Nyiragongo show significant ^{238}U-^{230}Th disequilibria but ($^{226}Ra/^{230}Th$) is in equilibrium indicating that these

lavas are either older than 8ka, but younger than 300 ka, or that their ($^{226}Ra/^{230}Th$) was in equilibrium when they erupted. As discussed below, the observation that several of the Nyirangongo lava samples show ($^{226}Ra/^{230}Th$) that is out of equilibrium limits the time span between the chemical fractionation (melting) that produced this disequilibria and eruption to be less than 8000 ky.

The young ages of the prehistoric lavas from Nyiragongo indicates rapid magma resurfacing rates. Apart from the two documented eruptions in 1977 and 2002, which were along fractures, the young age of the prehistoric lavas as well as the parasitic cones indicate that the frequency of Nyiragongo eruptions are higher than previously thought (Tazieff, 1995) and their mode of eruption (parasitic cones versus fractures flow) also varies. When compared with other global volcanoes, which have also erupted repeatedly in historic times, the high eruption frequency of Nyiragongo is not surprising. However, given the high population density around Nyiragongo, the high eruption-frequency and variable styles of eruptions (parasitic cones versus fracture flow) increases the hazard-potential of this volcano. Since the 1977 eruption, the potential impact of a volcanic eruption on inhabitants of Goma has increased manifold because of the mass exodus of Rwandan refugees to this region since the mid-1990s (Komorowski et al., 2002 - 2003). Given the wide-spread existence of refugee camps in and around Goma, a future eruption of Nyiragongo could create a humanitarian crisis of extreme proportions. The lava flow hazard of the Nyiragongo volcano on the surrounding regions has been recently modeled (Favalli et al., 2009; Chirico et al., 2009). However, these models only consider the N-S fracture flow but do not take into account the parasitic cones surrounding this area including the ones in downtown Goma many of which we have shown in this study to be

very young. Future hazard assessments need to consider the different styles of eruption of Nyiragongo. While the recorded eruptions of Nyiragongo have not caused many direct deaths, the unusually low-viscosity lavas are fast-moving and cause destruction of homes and infrastructure which significantly affects the local economy and well being. Other dangers associated with the Nyiragongo eruptions include ground emissions of carbon dioxide and acid rain associated with the extremely high sulfur dioxide emission (Carn, 2002-2003; Sawyer et al., 2008).

4.2. Petrogenesis of the Nyiragongo lavas: Evidence for a metasomatic source

Nyiragongo lavas are highly alkaline, trace element-enriched, and silica-undersaturated and their mineralogy is dominated by feldspathoidal phases (e.g. Sahama, 1960; Chakrabarti et al., 2009). Their unusual compositions differ even from the other volcanics of the Virunga Volcanic Province e.g. Nyamuragira (Aoki et al., 1985; Rogers et al., 1998; Chakrabarti et al., 2009) (Fig. 1b). The Nyiragongo volcanics show a wide range in ($^{230}Th/^{232}Th$) and ($^{238}U/^{232}Th$). However, most of the samples plot close to the equiline (Fig. 2), with some samples showing ^{230}Th excess and others showing ^{238}U excesses.

All of the Nyiragongo lavas analyzed in this study, and by Williams and Gill (1992), plot above the ($^{230}Th/^{232}Th$) versus $^{87}Sr/^{86}Sr$ hyperbolic array for oceanic basalts (MORB and OIB) as defined in Sims and Hart (2006) (Fig. 3). This is in contrast with basalts from the Kenya rift (Rogers et al., 2006) erupting in the Proterozoic mobile belt (MB) or remobilized cratonic margin (RCM), which plot below the array. Other continental alkaline rocks from around the world such as north-east China (Zou et al., 2003, 2008), Rio Grande rift in the south-west United States (Asmerom and Edwards, 1995; Reid, 1995; Reid and

290 Ramos, 1996; Asmerom, 1999, 2000; Sims et al., 2007), Mt. Erebus (Reagan et al., 1992;
291 Sims and Hart, 2006), and Gaussberg (Williams et al., 1992) in Antarctica, which despite
292 showing wide ranges in both Th and Sr isotopic ratios, plot on the "mantle array".

293 We interpret the high ($^{230}Th/^{232}Th$) in the Nyiragongo lavas relative to other mantle-
294 derived rocks as a two-stage process. In the first stage the source is metasomatically
295 enriched in ^{238}U. The second stage can only occur after a period of time significant enough
296 to allow for ^{230}Th ingrowth, hence it lying above the hyperbolic $^{87}Sr/^{86}Sr$ – ($^{230}Th/^{232}Th$)
297 array. Note that because of the 75ka half-life ^{230}Th, the time period required for ^{230}Th
298 ingrowth must be at least 10ka, which is equivalent to 1% uncertainty of ($^{230}Th/^{232}Th$) on a
299 U-Th isochron. This metasomatically ^{238}U enriched source is then partially melted to
300 produce the resulting erupted lavas. The observed variations in ($^{230}Th/^{232}Th$) and
301 ($^{238}U/^{232}Th$) in the Nyiragongo lavas suggest that the sources of these volcanics were not
302 uniformly metasomatized.

303 Several lines of evidence indicate that the metasomatic fluid affecting the source of
304 the Nyiragongo volcanics was carbonate-rich. Superchondritic Zr/Hf ratios (Jochum et al.,
305 1986) observed in the Nyiragongo lavas (Table 2) (Dupuy et al., 1992; Chakrabarti et al.,
306 2009) are indicative of carbonate metasomatism of their source, since in a co-existing
307 silicate-carbonate pair, Zr is more compatible in the carbonate phase compared to Hf
308 (Hamilton et al., 1989). This is documented by carbonatites distributed world-wide that
309 typically show high Zr/Hf (Andrade et al., 2002).

310 Carbonate-rich fluids are also enriched in U compared to Th (i.e. low Th/U) as is
311 clearly demonstrated by the low ($^{230}Th/^{238}U$), varying from 0.1-0.2, in natrocarbonatite
312 lavas from Oldoinyo Lengai in Tanzania (Pyle et al., 1991). As shown in a plot of

($^{230}Th/^{238}U$) versus Zr/Hf (Fig. 4), the Nyiragongo volcanics of the present study show a clear and variable imprint of carbonate metasomatism. This ($^{230}Th/^{238}U$) versus Zr/Hf correlation suggests that carbonate metasomatism in the mantle-source beneath the western rift influences U-Th disequilibria in these rocks. Quantitative modeling (Appendix 2), using primitive and carbonate-metasomatized mantle end-members from Campbell (2002) and Pyle et al. (1991), respectively, shows that the younger lavas of Nyiragongo, along with a few prehistoric lava samples, show >50-60% contribution of this carbonate metasomatized mantle source (Fig. 4), while most of the older Nyiragongo lavas show only 10-22% contribution of this source. This result suggests that carbonate metasomatism was not pervasive in the Nyiragongo, and possibly Virunga mantle-source, and/or the episode of metasomatism was relatively young. Although, the recent and some prehistoric lavas of Nyiragongo show as high as 60% contribution from a carbonate metasomatized mantle source, no discernible carbonate minerals have been identified in thin sections from a representative bigger sample set of the Nyiragongo lavas. The lack of carbonates in these lavas derived from a carbonate-metasomatized mantle-source maybe explained by the unusually high and persistent CO_2 flux of Nyiragongo (~ 21 Tg/yr) (Sawyer et al., 2008), which is much higher than other global volcanoes from different tectonic settings and showing wide ranging magma compositions (see Sawyer et al., 2008 and references therein).

It is important to note that the time interval between the fluid interaction in the mantle-source and the subsequent partial melting of this metasomatized source affects the position of an analyzed lava sample in the Sr-Th correlation diagram (Fig. 3). If this time interval is short compared to the half-life of ^{230}Th (~75 ky), and followed by ‘fast’ transport

of the partial melt, the Th isotopic ratio of the partial melt will not have time to grow into equilibrium with the enriched ^{238}U and thus represent that of the unmetasomatized mantle source, providing that the metasomatizing fluid had the same Th isotopic composition. If this is the case, then the sample may still lie on the mantle array in the Sr-Th isotopic diagram, although it may plot off the equiline with considerable ^{238}U excess [($^{230}Th/^{238}U$) <1]. The time required for ^{238}U-^{230}Th equilibrium to be restored is ~5 times the half-life of ^{230}Th (~300 ky). Thus our observation that the Nyiragongo volcanics have significant ($^{230}Th/^{238}U$) disequilibria and lie above the Sr-Th mantle-array (Fig. 3) indicates that this metasomatic event must have occurred <300 ky before eruption (necessary to maintain disequilibria), but long enough before eruption to ingrow ^{230}Th by the decay of ^{238}U).

($^{226}Ra/^{230}Th$) in the Nyiragongo lavas show an overall positive correlation with Zr/Hf, which is a proxy for carbonate metasomatism (Fig. 5). This indicates the role of carbonate metasomatism on the ($^{226}Ra/^{230}Th$) disequilibria observed in these samples. Our interpretation is consistent with the very high ($^{226}Ra/^{230}Th$) seen in carbonatites (Williams et al., 1986; Pyle et al., 1991), which are also characterized by high Zr/Hf (Andrade et al., 2002). Quantitative modeling (Appendix 2), using primitive-mantle (basanite) and carbonate-metasomatized mantle end-members (Williams et al., 1986) shows that the younger lavas of Nyiragongo, along with a few historic lava samples, show greater contribution of a carbonate metasomatized mantle end-member with 50-60% contribution while most of the older Nyiragongo lavas show only 2-22% contribution of this carbonate metasomatized source. These results are consistent to those obtained from modeling ($^{230}Th/^{238}U$) and Zr/Hf in these volcanics (Fig. 4). Based on this modeling, we estimate that

for the lavas with greater contribution from a carbonated mantle end-member, the time elapsed since partial melting is between 4-6 ka (Fig. 5).

Varying contribution of the carbonatitic end-member suggests that carbonate metasomatism beneath the Virunga volcanics was not pervasive and the mantle-source beneath these volcanics is not homogeneous. This is also supported by the relatively low Zr/Hf observed in the Nyamuragira volcanics (Chakrabarti et al., 2009), located only 15 km north of Nyiragongo, compared with much higher such values for Nyiragongo lavas.

4.2.2. Role of mineral fractionation and source mineralogy on U-Th-Ra disequilibria:

We interpret the U and Ra excess in some of the Nyiragongo lavas as an artifact of carbonate metasomatism in the source of these lavas. However, given the unusual mineralogy of these samples (e.g. Sahama, 1960, 1962, 1973; Chakrabarti et al., 2009), U-Th disequilibria in the Nyiragongo lavas could potentially be an artifact of mineral fractionation in the magma chamber or in the lava flow. The common micro-phenocrysts in the Nyiragongo volcanics are melilite, kalsilite, leucite, perovskite, Ti-augite and olivine which are hosted in a fine-grained glassy groundmass. Petrographically discernible groundmass minerals in the older lavas include kalsilite, nepheline, smaller amounts of leucite, and minor clinopyroxene, olivine, perovskite, apatite and titanomagnetite (Sahama, 1973). Large quantities of these aphyric rock samples (~15-20 grams) were crushed to obtain a compositionally representative powder for geochemical analyses and to minimize preferential isolation of minerals due to a "nugget effect". In addition, the smooth and uniform trace element patterns and narrow range of MgO, P_2O_5 and Mg# in all of these rock samples (Chakrabarti et al., 2009), also argue against mineral fractionation in the

magma chamber or in a lava flow causing the observed variability in U-Th-Ra disequilibria. It is important to note that separate dissolutions and analyses of powdered replicates of one sample (NY-37 and NY-37a) show ~ 4% variation suggesting slight heterogeneity in the sample powders.

Several minerals could potentially affect U-Th-Ra series disequilibria in the Nyiragongo lavas. Apatite is a minor groundmass component in the Nyiragongo lavas. However, the partition coefficients for Th and U are both close to unity for apatite/silicate melt although D_U shows greater variability compared to D_{Th} possibly due to slight changes in oxygen fugacity (Prowatke and Klemme, 2006). However, partition coefficients for Th and U decrease with decreasing silica contents in the melt (Prowatke and Klemme, 2006). Hence, we posit that apatite crystallization or residual apatite is not significantly affecting the Th/U ratio in the silica-undersaturated Nyiragongo lavas. U and Th are both incompatible in plagioclase with $D_U \sim 6 \times 10^{-4}$ and $D_{Th} \sim 4.6 \times 10^{-4}$ (Blundy and Wood, 2003). Although, D_{Ra} increases with sodium content in plagioclase, it is never greater than unity (Blundy and Wood, 2003). However, given the absence of any Eu-anomaly in the Nyiragongo lavas (Chakrabarti et al., 2009), plagioclase fractional crystallization in the source of these lavas can also be ruled out.

It is important to investigate whether the U-Th-Ra series disequilibria in the Nyiragongo lavas are influenced by their source mantle mineralogy. The Nyiragongo volcanics show high chondrite-normalized Dy/Yb ratios (1.7-2.0, Table 2) (Chakrabarti et al., 2009) indicating presence of residual garnet. U is more compatible in garnet compared to Th and hence small degrees of partial melting in the presence of residual garnet can fractionate Th/U. Partial melting in the presence of residual garnet results in large ^{230}Th

404 excess in the melt as observed in most oceanic basalts (Fig. 3) (Beattie, 1993; LaTourrette
405 et al., 1993; Sims et al., 1995; Stracke et al., 1999) which also show high chondrite-
406 normalized Dy/Yb ratios. While some of the Nyiragongo samples show slight ^{238}U excess
407 (Fig. 2), due to carbonate metasomatism of the source as discussed above, some of the
408 comparatively older Nyiragongo lavas clearly plot slightly to the left of the equiline (Fig. 2)
409 showing ^{230}Th excess. Based on this observation, it can be argued that two different
410 processes with opposite effects in terms of fractionating Th/U of the source must have
411 worked in tandem. One of these processes being metasomatism of the source as discussed
412 earlier while the other being partial melting in the presence of residual garnet.

413 Nyiragongo lavas are characterized by low K/Rb (~250) (Chakrabarti et al., 2009),
414 similar to phlogopite (Basu, 1978; Beswick, 1976) indicating derivation from a phlogopite-
415 bearing mantle source. Williams and Gill (1992) argue that melting of phlogopite, which
416 has high Th/U, can also result in ^{230}Th excess in the partial melt. Th and U are both equally
417 incompatible in phlogopite (LaTourrette et al., 1995). Hence, the Th/U of the melt would
418 reflect the Th/U of the phlogopite-bearing source. Therefore, partial melting of a carbonate
419 metasomatized phlogopite-bearing mantle source with residual garnet could explain why
420 the Nyiragongo volcanics plot on both sides of the equiline as shown in Figure 2. It can be
421 argued that Ra, which is geochemically similar to Ba, is compatible in phlogopite given the
422 high compatibility of Ba in phlogopite (D~30) (Blundy and Wood, 2003). Assuming
423 equilibrium porous flow the steady-state ($^{226}Ra/^{230}Th$) of phlogopite could be as high as 10-
424 100 (Feineman and DePaolo, 2003). Hence, melting of phlogopite would also result in high
425 ($^{226}Ra/^{230}Th$) in the melt consistent with the Ra-excess observed in some of the Nyiragongo
426 lavas. It must be mentioned that complete melting of the phlogopite in the mantle-source of

these rocks is critical; presence of any residual phlogopite would retain ^{226}Ra in the mantle resulting in a deficit of ^{226}Ra in the partial melt.

4.2.3. ^{210}Pb/^{226}Ra disequilibria in the Nyiragongo lavas

A couple of recent lava samples, one from the 2002 flow and the other from the 2003 lava lake were analyzed for ^{210}Pb. The 2003 lava lake shows ~10% (^{210}Pb) deficit relative to (^{226}Ra) whereas the initial (^{210}Pb/^{226}Ra) of the 2002 lava sample is in equilibrium (Table 2). Several processes can potentially fractionate Pb from Ra including partial melting, sulfide fractionation, and magma degassing as discussed below. Given the greater compatibility of Pb relative to Ra, melt generation can produce substantial ^{210}Pb deficits, as suggested for young MORB (Rubin et al., 2005) and Samoan lavas (Sims et al., 2008b). Pb is also highly chalcophilic and hence partial melting with residual sulfides can result in ^{210}Pb deficits. However, there is no available data suggesting the presence of residual sulfide in the Nyiragongo source. In addition, average Pb concentration in these samples is reasonably high (6.2 ppm) (Chakrabarti et al., 2009), which also precludes the presence of residual sulfide in the source of the Nyiragongo lavas.

Alternatively, while Pb is only slightly volatile, continuous degassing of the intermediate daughter ^{222}Rn can create large ^{210}Pb deficits in magmas (Gauthier and Condomines, 1999; Turner et al., 2004; Reagan et al., 2006, 2008; Sims and Gauthier, 2007; Sims et al., 2008b). The concentration of ^{222}Rn is extremely low in magmas and hence it needs another carrier gas (e.g. CO_2, SO_2, H_2O etc.) to be extracted and degassed from a magma (Gauthier and Condomines, 1999; Giammanco et al., 2007). Compared to H_2O and SO_2, CO_2 degasses at comparatively greater depths due to its lower solubility. It

450 has been suggested that ^{222}Rn extracted along with CO_2 at greater depths is likely to decay
451 in-situ before eruption and hence does not affect the ($^{210}Pb/^{226}Ra$) of the magma; hence
452 efficient Rn degassing occurs only at shallower depths, mainly through exsolution of SO_2
453 and H_2O (Gauthier and Condomines, 1999) In contrast, positively correlated high ^{222}Rn
454 activity and CO_2 flux in Mt. Etna argues for deeper degassing of Rn (Giammanco et al.,
455 2007).

456 We suggest that the moderate deficit of ^{210}Pb with respect to ^{226}Ra in the 2003 lava
457 lake sample likely reflects the persistent loss of ^{222}Rn for years to decades by its
458 partitioning into a gas phase. This Rn-loss could have occurred as the magma rose to the
459 surface from the mantle as well as during its one-year residence in the lava lake, which was
460 reestablished after the 2002 eruption and is noted for its persistent gas plume (see Sawyer
461 et al., 2008). If all radon in our sample of the lava lake was persistently lost, then its total
462 duration of gas-loss and residence in the conduit system and lake could have been as little
463 as 3 years. Significantly longer degassing times are allowed if Rn-loss was less efficient.
464 For example, if only 1/10 of the radon was persistently lost, then magma degassing
465 residence times could have been greater than a century (see Gauthier and Condomines,
466 1999). If similar ^{210}Pb-^{226}Ra disequilibrium marked the parental magma for sample NY-1-
467 02, then this magma ceased degassing for at least a decade while it resided in the shallow
468 reservoir system of Nyiragongo before it erupted.
469

470 **5. Conclusions**

471 Our measurements of ^{238}U-^{230}Th-^{226}Ra-^{210}Pb provide insight into the timescales and
472 nature of magmatic processes occurring beneath Nyiragongo. Recent lava samples from

2002 and 2003 and three other prehistoric lava samples of Nyiragongo show ($^{226}Ra/^{230}Th$) disequilibria limiting the eruption ages of these prehistoric lavas to be less than 8 ka. Five other prehistoric lava samples show significant ^{238}U-^{230}Th disequilibria but with ($^{226}Ra/^{230}Th$) equal to unity indicating that they were erupted between 8-300 ka. Quantitative modeling suggests that for these samples, the time elapsed since partial melting is 4-6 ka. $^{226}Ra/^{230}Th$ disequilibria in the Nyiragongo lavas, as presented in this study implies that rate of magma upwelling, from melting in the source mantle to its eruption on the surface, is much less than 8000 ky.

The ^{210}Pb-^{226}Ra observed for the 2003 lava lake sample suggests that its parental magma had a few year- to several decade-long period of degassing as it rose from the mantle and while it resided in the lava lake. In contrast, the 2002 lava represented by sample NY-1-02 appears to have stagnated in the reservoir system and ceased degassing for a decade or more before it erupted.

To explain both significant ^{230}Th excesses [($^{230}Th/^{238}U$) > 1] and ^{238}U excesses [($^{230}Th/^{238}U$) < 1] in the Nyiragongo lavas, we hypothesize that different processes are working in concert to generate the observed range of disequilibria. These processes include, both: 1) low degree partial melting of the mantle source containing residual garnet (consistent with the super-chondritic Dy/Yb in these lavas) and phlogopite (consistent with their low K/Rb ratios) to produce the observed ^{230}Th excesses; and, 2) ^{238}U enrichment due to carbonate metasomatism (consistent with the high Zr/Hf in the Nyiragongo lavas). Our proposed model of partial melting of a garnet and phlogopite-bearing carbonate-metasomatized mantle source is consistent with observed trends between ($^{230}Th/^{232}Th$) versus $^{87}Sr/^{86}Sr$, and ($^{230}Th/^{238}U$) and ($^{226}Ra/^{230}Th$) versus Zr/Hf.

Carbonate metasomatism in the source of the Nyiragongo volcanics took place <300 ky ago resulting in ($^{230}Th/^{232}Th$) higher than those observed in most mantle-derived rocks, especially ocean-island basalts. The rough correlation between ($^{226}Ra/^{230}Th$) and Zr/Hf along with quantitative modeling suggests that the 2002 and 2003 lavas and a few older lava samples must have incorporated 50-60% of a carbonate-metasomatized mantle source while the older lavas included only 10-22% of this source. This result indicates that carbonate-metasomatism in the mantle source of Nyiragongo was not pervasive and the mantle source beneath Nyiragongo (and possibly entire Virunga) is not homogeneous, consistent with radiogenic isotope data from Chakrabarti et al. (2009).

Acknowledgements:

This paper is dedicated to the memory of co-author Jacques Durieux (1949-2009), who had a profound geological insight for this area and a love for Nyiragongo. Lava samples were collected as a part of a field work in Nyiragongo, supported by UN-OCHA grants. The field team included Paolo Papale, Alba Santo, Dario Tedesco and Orlando Vaselli with support from the staff of Goma Volcanological Observatory, D. R. Congo. The 2003 lava lake sample was collected by Jacques Durieux. Funding for U-series analyses was covered by NSF-EAR 063824101 and NSF-EAR 083887800 to KWWS. ^{210}Po analyses were funded with EAR0738776 to MR. Sample preparation and dissolution was covered by NSF-EAR 0732679 to ARB. RC acknowledges guest student award from WHOI. We would like to thank two anonymous reviewers, Rick Carlson and Dario Tedesco for their comments and suggestions.

Figure Captions:

Figure 1. (a) Simplified map showing the major structures of the East African Rift System and location of the Virunga Volcanic Province (VVP) (black triangle). **(b)** Different volcanoes of the VVP including Nyiragongo of the present study. **(c)** Geological map of the Nyiragongo volcanic complex showing several plugs, cones, and the lava plane as well as the locations of the samples of the present study (filled circles, see Table 1). Also shown are the Nyamuragira and Karisimbi volcanic planes.

Figure 2. Plot of the activity ratios of $^{230}Th/^{232}Th$ versus $^{238}U/^{232}Th$ (shown in parenthesis) for the Nyiragongo lavas of this study (filled circles, N=13). Our results overlap with previous analyses of the Nyiragongo lavas by Williams and Gill (1992) (open circles) but are strikingly different from those of Tedesco et al. (2007) (not plotted) who reported much higher ($^{238}U/^{232}Th$) ranging from 1.5-2.81. Also shown for comparison are the fields of oceanic basalts (see Sims and Hart, 2006) and continental alkaline volcanics from south-west United States (Asmerom and Edwards, 1995; Asmerom, 1999; Asmerom et al., 2000), Gaussberg (Williams et al., 1992), Mt. Erebus (Sims and Hart, 2006), Wudalianchi (Zou et al., 2003, 2008) and Kenya rift with different basement types (Remobilized cratonic margin or RCM and the late Proterozoic mobile belt or MB) (Rogers et al., 2006). The Nyiragongo lavas plot near to but on both sides of the equiline showing U-Th disequilibria.

Figure 3. Correlation between ($^{230}Th/^{232}Th$) and the $^{87}Sr/^{86}Sr$. The array defined by oceanic basalts (Sims and Hart, 2006) is shown by the shaded region. Also plotted for comparison are other global continental alkaline volcanics (See Figure 2 caption for details). Nyiragongo lavas of this study (filled circles, N=13) overlap with the analyses of Williams and Gill (1992) (open circles) and lie above this array. The enrichment of ^{230}Th in Nyiragongo relative to other mantle-derived rocks suggests enrichment of the source in ^{238}U and a significant time difference between the metasomatic enrichment and partial melting to allow growth of ^{230}Th.

Figure 4. Nyiragongo volcanics of the present study show a rough negative correlation between ($^{230}Th/^{238}U$) and Zr/Hf, a proxy for carbonate metasomatism, suggesting that carbonate metasomatism in the mantle-source beneath Virunga resulted in ^{238}U excess seen some of these rocks. Our forward modeling results indicate that the youngest Nyiragongo lavas and some historic lava samples were derived from a mantle-source with 50-60% contribution from a carbonatitic end-member while the other historic lavas show up to 20% mixing of a carbonatitic mantle-end member with a primitive mantle end-member. Parameters for the carbonatitic end-member are from Pyle et al. (1991) and some of the parameters for the primitive mantle are from Cambell (2002) and Jochum et al. (1986). Parameters for our best-fit model are as follows: Th/U (carbonatite) = 0.3, Th/U (primitive mantle) = 4.04, Zr/Hf (Carbonatite) = 100, Zr/Hf (primitive mantle) = 38, ($^{230}Th/^{238}U$) (carbonatite) = 0.11and ($^{230}Th/^{238}U$) (primitive mantle) = 1.05

Figure 5. Activity of $^{226}Ra/^{230}Th$ for the Nyiragongo volcanics shows an overall positive correlation with Zr/Hf (inset), a proxy for carbonate metasomatism, suggesting contribution from a carbonate-metasomatized source. Our forward modeling results indicates that younger lavas (black circles) and some of the older unknown-age lava samples (gray circles) show greater contribution (50-60%) from a carbonated mantle component whereas most of the older unknown-age lavas show lesser contribution (2-22%) of this component consistent with our modeling results using ($^{230}Th/^{238}U$) and Zr/Hf as shown in Figure 4.. Our data, however, plot below a simple mixing curve between the above-mentioned end-members. This is an artifact of the time elapsed since partial melting of this mixed source, which produced the Nyiragongo lavas. The lavas with higher Zr/Hf must have erupted within 4-6 ky since partial melting. Parameters for the carbonatitic end-member are from Williams et al. (1986) and Jochum et al. (1986). Mantle values are from our analyses of basanite lavas from Nyamuragira (Chakrabarti et al., 2009), which will be reported in a different study. Parameters for our best-fit model are as follows: Ra/Th (Carbonatite) = 0.044, Ra/Th (primitive mantle) = 0.008, Zr/Hf (Carbonatite) = 100, Zr/Hf (primitive mantle) = 38, ($^{226}Ra/^{230}Th$) (carbonatite) = 2.07 and ($^{226}Ra/^{230}Th$) (primitive mantle) = 1.02

References

Andrade, F.R.D.D., Moller, P. and Dulski, P., 2002. Zr/Hf in carbonatites and alkaline rocks: new data and a re-evaluation. Revista Brasileira de Geociencias, 32(3): 361-370.

585 Aoki, K., Yoshida, T., Yusa, K. and Nakamura, Y., 1985. Petrology and geochemistry of
586 the Nyamuragira volcano, Zaire. Journal of volcanology and Geothermal research,
587 25(1-2): 261-265.
588 Asmerom, Y., 1999. Th–U fractionation and mantle structure Earth and Planetary
589 Science Letters, 166 163–175.
590 Asmerom, Y., Cheng, H., Thomas, R., Hirschmann, M. and Edwards, R.L., 2000.
591 Melting of the Earth's lithospheric mantle inferred from protactinium±
592 thorium±uranium isotopic data. Nature, 406: 293-296.
593 Asmerom, Y. and Edwards, R.L., 1995. U-series isotope evidence for the origin of
594 continental basalts. Earth and Planetary Science Letters, 134: l-7.
595 Baker, B. H., Williams, L.A.J., Miller J.A. and Fitch F.J., 1971. Sequence and
596 geochronology of the Kenya rift volcanics. Tectonophysics, 11:191-215.
597 Ball, L., Sims, K.W.W. and Schwieters, J., 2008. Measurement of 234U/238U and
598 230Th/232Th in volcanic rocks using the NEPTUNE PIMMS. Journal of
599 Analytical and Atomic Spectroscopy, 23: 173-180, doi:10.1039/b703193a.
600 Basu, A.R., 1978. Trace-elements and Sr-isotopes in some mantle-derived hydrous
601 minerals and their significance. Geochimica et Cosmochimica Acta, 42(NA6):
602 659-668.
603 Baxter, P. et al., 2002-2003. Human health and vulnerability in the Nyiragongo volcano
604 eruption and humanitarian crisis at Goma, Democratic Republic of Congo. Acta
605 Vulcanologica, 14(1-2) - 15(1-2): 109-114.
606 Beattie, P., 1993. Uranium-thorium disequilibria and partitioning on melting of garnet
607 peridotite. Nature, 363: 63-65.

608 Beswick, A.E., 1976. K and Rb relations in basalts and other mantle derived materials. Is
609 phlogopite the key? Geochimica et Cosmochimica Acta, 40: 1167-1183.
610 Blundy, J. and Wood, B., 2003. Mineral-melt partitioning of Uranium, Thorium and their
611 daughters. In: B. Bourdon, G.M. Henderson, C.C. Lundstrom and S.P. Turner
612 (Editors), Reviews in mineralogy and geochemistry: Uranium series
613 geochemistry, pp. 59-118.
614 Bourdon, B., Goldstein, S., Bourles, D., Murrell, M.T. and Langmuir, C.T., 2000.
615 Evidence from 10Be and U series disequilibria on the possible contamination of
616 mid-oceanic ridge basalt glasses by sedimentary material. Geochemistry,
617 Geophysics, Geosystems, 1(8): doi:10.1029/2000GC000047.
618 Campbell, I.H., 2002. Implications of Nb/U, Th/U and Sm/Nd in plume magmas for the
619 relationship between continental and oceanic crust formation and the development
620 of the depleted mantle. Geochimica et Cosmochimica Acta, 66(9): 1651-1661.
621 Carn, S.A., 2002-2003. Eruptive and passive degassing of sulphur dioxide at Nyiragongo
622 volcano (D. R. Congo): The 17th January 2002 eruption and its aftermath. Acta
623 Vulcanologica, 14 (1-2) - 15(1-2): 75-86.
624 Chakrabarti, R., Basu, A.R., Santo, A.P., Tedesco, D. and Vaselli, O., 2009. Isotopic and
625 Geochemical study of the Nyiragongo and Nyamuragira volcanics in the western
626 rift of the East African rift system. Chemical Geology, 259: 273-289.
627 Chirico, G. D., Favalli, M., Papale, P., Boschi, E., Pareschi, M. T. and Mamou-Mani, A.
628 2009, Lava flow hazard at Nyiragongo Volcano, DRC. 2. Hazard reduction in
629 urban areas, Bulletin of Volcanology 71 (4), 375-387

630 Dawson, J. B., Pinkerton, H., Norton, G. E. and Pyle, D. M., 1990. Physiochemical
631 properties of alkali carbonatite lavas: Data from the 1988 eruption of Oldoinyo
632 Lengai, Tanzania. Geology, 18: 260-263.
633 Demant, A., Lestrade, P., Lubala, R.T., Kampunzu, A.B. and Durieux, J., 1994.
634 Volcanological and Petrological evolution of Nyiragongo Volcano, Virunga
635 volcanic field, Zaire. Bulletin of Volcanology, 56(1): 47-61.
636 Dupuy, C., Liotard, J.M. and Dostal, J., 1992. Zr/Hf fractionation in intraplate basaltic
637 rocks: Carbonate metasomatism in the mantle source. Geochimica et
638 Cosmochimica Acta, 56: 2417-2423.
639 Durieux, J., 2002-2003. Nyiragongo: The January 10th 1977 eruption. Acta
640 Vulcanologica, 14 (1-2) - 15 (1-2): 145-148.
641 Favalli, M., Chirico, G. D., Papale, P., Pareschi, M. T. and Boschi, E., 2009, Lava flow
642 hazard at Nyiragongo Volcano, DRC. 1. Model calibration and hazard mapping,
643 Bulletin of Volcanology 71 (4), 363-374
644 Feineman, M.D. and DePaolo, D.J., 2003. Steady-state 226Ra/230Th disequilibrium in
645 mantle minerals: Implications for melt transport rates in island arcs. Earth and
646 Planetary Science Letters, 215: 339-355.
647 Furman, T., 2007. Geochemistry of East African Rift basalts: An overview. Journal of
648 African Earth Sciences 48(2-3): 147-160.
649 Gauthier, P.-M. and Condomines, M., 1999. Pb-Ra radioactive disequilibria in recent
650 lavas and radon degassing: inferences on the magma chamber dynamics at
651 Stromboli and Merapi volcanoes. Earth and Planetary Science Letters, 172: 111-
652 126.

653 Giammanco, S., Sims, K.W.W. and Neri, S.M., 2007. Shallow rock stresses and gas
654 transport at Mt. Etna (Italy) monitored through ^{220}Rn, ^{222}Rn and soil CO_2
655 emissions in soil and fumaroles. Geochemistry, Geophysics and Geosystems, 8:
656 Q10001, doi:1029/2007GC00164
657 Giordano, D. et al., 2007. Thermo-rheological magma control on the impact of highly
658 fluid lava flows at Mt. Nyiragongo. Geophysical Research Letters, 34: L06301,
659 doi:10.1029/2006GL028459.
660 Goldstein, S. J., Murrell, M. T., Janecky, D. R., Delaney, J. R. and Clague, D. A., 1991.
661 Geochronology and petrogenesis of MORB from the Juan de Fuca and Gorda
662 ridges by ^{238}U and ^{230}Th disequilibrium. Earth and Planetary Science Letters, 107:
663 25-41.
664 Goldstein, S. J., Perfit, M. R., Batiza, R., Fornari, D. J. and Murrell, M. T., 1994. Off-axis
665 volcanism at the East Pacific Rise detected by uranium-series dating of basalts.
666 Nature, 367: 157-159.
667 Hamilton, D.L., Bedson, P. and Esson, J., 1989. The behavior of trace elements in the
668 evolution of Carbonatites. In: K. Bell (Editor), Carbonatites: genesis and
669 evolution. Unwin Hyman, London, Boston, pp. 405-427.
670 Holmes, A. and Harwood, F., 1937. The petrology of the volcanic area of Bufumbira.
671 Geological Survey of Uganda Memoir, 3.
672 Jochum, K.P., Seufert, M.H., Spettel, B. and Palme, H., 1986. The solar system
673 abundances of Nb, Ta and Y and the relative abundances of refractory lithophile
674 elements in differentiated planetary bodies. Geochimica et Cosmochimica Acta,
675 50: 1173-1183.

676 Komorowski, J.-C. et al., 2002 - 2003. The January 2002 flank eruption of Nyiragongo
677 volcano (Democratic Republic of Congo): Chronology, evidence for a tectonic rift
678 trigger, and impact of lava flows on the city of Goma. Acta Vulcanologica, 14(1-
679 2) - 15(1-2): 27-62.
680 LaTourrette, T., Hervig, R.L. and Holloway, J.R., 1995. Trace element partitioning
681 between amphibole, phlogopite and basanite melt. Earth and Planetary Science
682 Letters, 135: 13-30.
683 LaTourrette, T.Z., Kennedy, A.K. and Wasserburg, G.J., 1993. Thorium-Uranium
684 Fractionation by Garnet: Evidence for a Deep Source and Rapid Rise of Oceanic
685 Basalts. Science, 261.
686 Pik, R., Deniel, C., Coulon, C., Yirgu, G. and Marty, B., 1999. Isotopic and trace element
687 signatures of Ethiopian flood basalts: evidence for plume-lithosphere interactions.
688 Geochimica et Cosmochimica Acta, 63: 2263-2279.
689 Pik, R., Marty, B. and Hilton, D.R., 2006. How many mantle plumes in Africa? The
690 geochemical point of view. Chemical Geology, 226: 100-114.
691 Platz, T., Foley, S.F. and Andre, L., 2004. Low-pressure fractionation of the Nyiragongo
692 volcanic rocks, Virunga Province, D. R. Congo. Journal of Volcanology and
693 Geothermal research, 136: 269-295.
694 Prowatke, S. and Klemme, S., 2006. Trace element partitioning between apatite and
695 silicate melts. Geochimica et Cosmochimica Acta, 70: 4513-4527.
696 Pyle, D.M., Dawson, J.B. and Ivanovich, M., 1991. Short-lived decay series equilibria in
697 the natrocarbonatite lavas of Oldoinyo Lengai, Tanzania: constraints on the
698 timing of magma genesis. Earth and Planetary Science Letters, 105: 378-396.

699 Reagan, M.K., Volpe, A.M. and Cashman, K.V., 1992. ^{238}U- and ^{232}Th-series chronology
700 of phonolite fractionation at Mount Erebus, Antarctica. Geochimica et
701 Cosmochimica Acta, 56: 1401-1407.
702 Reagan, M.K., Tepley, F.J., Gill, J., Wortel, M. and Hartman, B., 2005. Rapid timescales
703 of basalt to andesite differentiation at Anatahan volcano, Mariana Islands. Journal
704 of Volcanology and Geothermal research, 146: 171-183.
705 Reagan, M.K., Tepley III, F.J., Gill, J.B., Wortel, M. and Garrison, J., 2006. Timescales
706 of degassing and crystallization implied by ^{210}Po-^{210}Pb-^{226}Ra disequilibria for
707 andesitic lavas erupted from Arenal volcano. Journal of Volcanology and
708 Geothermal research, 157: 135-146.
709 Reagan, M.K., Cooper, K.M., Pallister, J.S., Thornber, C.R. and Wortel, M., 2008.
710 Timing of degassing and plagioclase growth in lavas erupted from Mount St.
711 Helens, 2004–2005, from ^{210}Po-^{210}Pb-^{226}Ra disequilibria,. In: D.R. Sherrod, W.E.
712 Scott and P.H. Stauffer (Editors), A Volcano Rekindled: The First Year of
713 Renewed Eruption at Mount St. Helens, 2004–2006. U.S. Geological Survey
714 Professional Paper.
715 Reid, M.R., 1995. Processes of mantle enrichment and magmatic differentiation in the
716 eastern Snake River Plain: Th isotope evidence. Earth and Planetary Science
717 Letters, 131: 239-254.
718 Reid, M.R. and Ramos, F.C., 1996. Chemical dynamics of enriched mantle lithosphere in
719 the southwestern U.S.: Th isotope evidence. Earth and Planetary Science Letters,
720 138: 67-81.

721 Rogers, N.W., James, D., Kelley, S.P. and DeMulder, M., 1998. The generation of
722 potassic lavas from the eastern Virunga province, Rwanda. Journal of Petrology,
723 39: 1223-1247.
724 Rogers, N.W., Thomas, L.E., Macdonald, R., Hawkesworth, C.J. and Mokadem, F.,
725 2006. ^{238}U-^{230}Th disequilibrium in recent basalts and dynamic melting beneath the
726 Kenya rift. Chemical Geology, 234: 148-168.
727 Rubin, K.H. and Macdougall, J. D., 1990. Dating of neovolcanic MORB using
728 (^{226}Ra/^{230}Th) disequilibrium. Earth and Planetary Science Letters, 101:313-322.
729 Rubin, K.H., Macdougall, J. D. and Perfit, M. R., 1994. ^{210}Po-^{210}Pb dating of recent
730 volcanic eruptions on the seafloor. Nature, 368: 841-844
731 Rubin, K.H., van der Zander, I., Smith, M.C. and Bergmanis, E.C., 2005. Minimum
732 speed limit for ocean ridge magmatism from ^{210}Pb-^{226}Ra-^{230}Th disequilibria.
733 Nature, 437: 534-538.
734 Sahama, T.G., 1960. Kalsilite in the lavas of Mount Nyiragongo (Belgian Congo).
735 Journal of Petrology, 1(2): 146-171.
736 Sahama, T.G., 1962. Petrology of Mt. Nyiragongo: a review. Transactions of the
737 Edinburgh Geological Society, 19(1): 1-28.
738 Sahama, T.G., 1973. Evolution of the Nyiragongo Magma. Journal of Petrology, 14(1):
739 33-48.
740 Sahama, T.G. and Smith, V.J., 1957. Tri-kalsilite, a new mineral. American Mineralogist,
741 42: 286.

742 Sawyer, G.M., Carn, S.A., Tsanev, V.I., Oppenheimer, C. and Burton, M., 2008.
743 Investigation into magma degassing at Nyiragongo volcano, Democratic Republic
744 of the Congo. Geochemistry Geophysics Geosystems, 9(2): -.
745 Schilling, J.-G., Kingsley, R.H., Hanan, B.B. and McCully, B.L., 1992. Nd-Sr-Pb
746 isotopic variations along the Gulf of Eden: evidence for Afar mantle plume-
747 continental lithosphere interactions. Journal of Geophysical Research, 97: 10297-
748 10966.
749 Sims, K.W.W. et al., 2003. Aberrant Youth: Chemical and isotopic constraints on the
750 young off-axis lavas of the East Pacific Rise. Geochemistry, Geophysics and
751 Geosystems, 4(10): 8621,doi:10.1029/2002GC000443.
752 Sims, K.W.W.S., DePaolo, D. J., Murrell, M. T., Baldridge, W.S., Goldstein, S.J. and
753 Clague, D. A. 1995. Mechanisms of magma generation beneath Hawaii and Mid–
754 Ocean ridges: U–Th and Sm–Nd isotopic evidence. Science, 267: 508–512.
755 Sims, K.W.W. and Gauthier, P.-J., 2007. From source to surface: U-series constraints on
756 the processes and timescales of magma generation, evolution and degassing,
757 International conference on Evolution, Transfer and Releases of Magmas and
758 Volcanic Gases. Acad. Sin., Taipei.
759 Sims, K.W.W.S., et al., 2008a. An inter-laboratory assessment of the Th Isotopic
760 Composition of Synthetic and Rock standards. Geostandards and Analytical
761 Research, 32(1): 65-91.
762 Sims, K.W.W. and Hart, S.R., 2006. Comparison of Th, Sr, Nd and Pb isotopes in
763 oceanic basalts: Implications for mantle heterogeneity and magma genesis. Earth
764 and Planetary Science Letters, 245 743–761.

765 Sims, K.W.W., Reagan, M. K., Blusztajn, J., Staudigel, H., Sohn, R. A., Layne, G. D.,
766 Ball, L. A. and Andrews, J., 2008b. ^{238}U-^{230}Th-^{226}Ra-^{210}Pb-^{210}Po, ^{232}Th-^{228}Ra, and
767 ^{235}U-^{231}Pa constraints on the ages and petrogenesis of Vailulu'u and Malumalu
768 Lavas, Samoa. Geochemistry, Geophysics, Geosystems, 9(4):
769 Q04003,doi:10.1029/2007GC001651.
770 Sims, K.W.W., Ackert, R. P., Ramos, F. C., Sohn, R. A., Murrell, M. T. and DePaolo, D.
771 J., 2007. Determining eruption ages and erosion rates of Quaternary basaltic
772 volcanism from combined U-series disequilibria and cosmogenic exposure ages.
773 Geology, 35(5): 471-474.
774 Sims, K. W. W. et al., 1999. Porosity of the melting zone and variations in solid mantle
775 upwelling rate beneath Hawaii: Inferences from 238U-230Th-226Ra and 235U-
776 231Pa disequilibria. Geochimica et Cosmochimica Acta, 63: 4119-4138.
777 Sims, K. W. W. et al., 2002. Chemical and isotopic constraints on the generation and
778 transport of magma beneath the East Pacific Rise. Geochimica et Cosmochimica
779 Acta, 66: 3481-3504.
780 Stracke, A., Salters, V.J.M. and Sims, K.W.W., 1999. Assessing the role of pyroxenite in
781 the source of Hawaiian basalts: Hf-Nd-Th isotope evidence. Geochemistry,
782 Geophysics, Geosystems, 1(1999GC0000013).
783 Sun, S.-s. and McDonough, W.F., 1989. Chemical and isotopic systematics of oceanic
784 basalts: implications for mantle composition and processes. Magmatism in the
785 Ocean Basins, Geological Society Special Publication, 42: 313-345.
786 Tazieff, H., 1995. Volcanic risk for Rwandan refugees. Nature, 376: 394.

787 Tedesco, D., Vaselli, O., Papale, P., Carn, S. A., Voltaggio, M., Sawyer, G. M., Durieux,
788 J., Kasereka, M. and Tassi, F., 2007. January 2002 volcano-tectonic eruption of
789 Nyiragongo volcano, Democratic Republic of Congo. Journal of Geophysical
790 Research, 112, (B09202): 10.1029/2006JB004762.
791 Turner, S.P., Black, S. and Berlo, K., 2004. ^{210}Pb-^{226}Ra and ^{226}Ra-^{230}Th systematics in
792 young arc lavas: Implications for magma degassing and ascent rates. Earth and
793 Planetary Science Letters, 227: 1-16.
794 Vanlerberghe, L., Hertogen, J. and MacDougall, J.D., 1987. Geochemical evolution and
795 Th-U isotope systematics of alkaline lavas from Nyiragongo volcano (African
796 rift). Terra Cognita, 7: 367.
797 Williams, R.W., Collerson, K.D., Gill, J.B. and Deniel, C., 1992. High Th/U ratios in
798 subcontinental lithospheric mantle: mass spectrometric measurement of Th
799 isotopes in Gaussberg lamproites. Earth and Planetary Science Letters, 111: 257-
800 268.
801 Williams, R.W. and Gill, J.B., 1992. Th isotope and U-series disequilibria in some alkali
802 basalts. Geophysical Research Letters, 19(2): 139-142.
803 Williams, R.W., Gill, J.B. and Bruland, K.W., 1986. Ra-Th disequilibria systematics:
804 Time of carbonatite magma formation at Oldoinyo Lengai volcano, Tanzania.
805 Geochimica et Cosmochimica Acta, 50: 1249-1259.
806 Zou, H., Fan, Q. and Yao, Y., 2008. U–Th systematics of dispersed young volcanoes in
807 NE China: Asthenosphere upwelling caused by piling up and upward thickening
808 of stagnant Pacific slab. Chemical Geology, 255: 134-142.

809 Zou, H. et al., 2003. Constraints on the origin of historic potassic basalts from northeast
810 China by U–Th disequilibrium data. Chemical Geology, 189-201.
811
812
813

Table 1. Brief description of the Nyiragongo lava samples of the present study including the GPS coordinates of the samples for which the information is available (See Figure 1).

Sample#	Location/Description	Lat/Long
NY-36	Rutoke cone	01°34'37.3" S 29°10'47.4" E
NY-37	Rushayo old lava	01°34'42.8" S 29°10'47.4" E
NY-37a	Rushayo old lava	01°34'42.8" S 29°10'47.4" E
NY-39	Mugara cone	01°37'17.6" S 29°15'11.0" E
NY-44	Buhuma cone	01°35'46.2" S 29°16'13.5" E
NY-53	Nyamushawa cone (bottom of crater)	01°30'19.9" S 29°18'59.4" E
NY-57	Ciraba cone	01°30'08.9" S 29°19'26.7" E
NY-66	Top of the main Nyiragongo crater	
NY-68	First lava flow of Shaheru	
NY-1-02	2002 lava flow of Nyiragongo	
NY-5-02	2002 lava flow of Nyiragongo	
NY-23-02	2002 lava flow of Nyiragongo	
2003 lavalk	2003 lava lake of Nyiragongo	

Table 2. U, Th concentrations (ID) and ^{238}U-^{230}Th-^{226}Ra-^{210}Pb disequilibria data for the Nyiragongo volcanics. Internal precision (2σ) is much less than 1% for (^{230}Th/^{232}Th). However, when propagated uncertainties related to tail correction are included, the errors are ~ 1% for (^{230}Th/^{232}Th). The error for ^{238}U and ^{232}Th concentration determination are ~0.5-1% based on both internal precision and uncentrainties in spike calibration and propagated errors for (^{238}U/^{232}Th) are 1-2 %. For some samples (e.g. NY-37a) the external reproducibility on separate powder dissolutions is ~ 4% for (^{230}Th/^{238}U) and (^{226}Ra/^{230}Th). For Ra measurements, internal precision is 1-2 % similar to the uncertainties in the ^{228}Ra spike calibration and the NIST ^{226}Ra standard against which the spike was calibrated. 2σ errors for ^{210}Po measurements are shown. Sr isotopic data, Zr/Hf and chondrite-normalized Dy/Yb for the samples are from Chakrabarti et al. (2009).

	U (ppm)	Th (ppm)	Th/U	(^{238}U/^{232}Th)	(^{230}Th/^{232}Th)	(^{230}Th/^{238}U)	^{226}Ra (dpm/g)	(^{226}Ra/^{230}Th) blank av.	^{210}Po ± 2σ (dpm/g)	(^{210}Pb/^{226}Ra) initial	^{87}Sr/^{86}Sr	Zr/Hf	Dy/Yb$_{(N)}$
NY-36	4.36	10.63	2.44	1.24	1.36	1.09	3.51	1.00			0.704382	48	2.00
NY-37	5.26	15.54	2.95	1.03	1.11	1.08	4.30	1.02			0.704431	53	1.74
NY-37a	4.90	13.76	2.81	1.08	1.11	1.03							
NY-39	5.37	13.83	2.58	1.18	1.24	1.05	4.18	1.00			0.704485	42	1.72
NY-44	2.76	8.29	3.00	1.01	1.04	1.03	2.10	1.00			0.704737	40	1.74
NY-53	3.95	10.58	2.68	1.13	1.10	0.97	2.84	1.00			0.704518	47	1.81
NY-57	7.03	17.27	2.46	1.23	1.19	0.97	5.62	1.12			0.704554	73	1.74
NY-66	9.45	22.01	2.33	1.30	1.23	0.94	7.20	1.09			0.704587	73	1.74
NY-68	9.66	22.32	2.31	1.31	1.26	0.96	7.42	1.08				74	1.72
NY-1-02	9.60	22.03	2.29	1.32	1.26	0.95	7.36	1.09	7.27 ± 0.32	0.99	0.704690	69	1.79
“									7.51 ± 0.28	1.03			
“									7.57 ± 0.30	1.04			
NY-5-02	9.63	22.41	2.33	1.30	1.26	0.97	7.29	1.06			0.704674	75	1.88
NY-23-02	9.60	20.71	2.16	1.41	1.26	0.90	7.17	1.12			0.704608	75	1.80
2003 lava lake	9.20	21.42	2.33	1.30	1.25	0.96	6.98	1.07	6.38 ± 0.22	0.90		75	1.74
“									6.54 ± 0.22	0.92			
ATHO	2.25	7.40	3.29	0.92	1.01	1.10	1.82	1.00					
TML	10.52	29.52	2.80	1.08	1.08	1.00	7.82	1.00					
BCR-2	1.69	5.86	3.46	0.88	0.87	1.00	1.26	1.01					

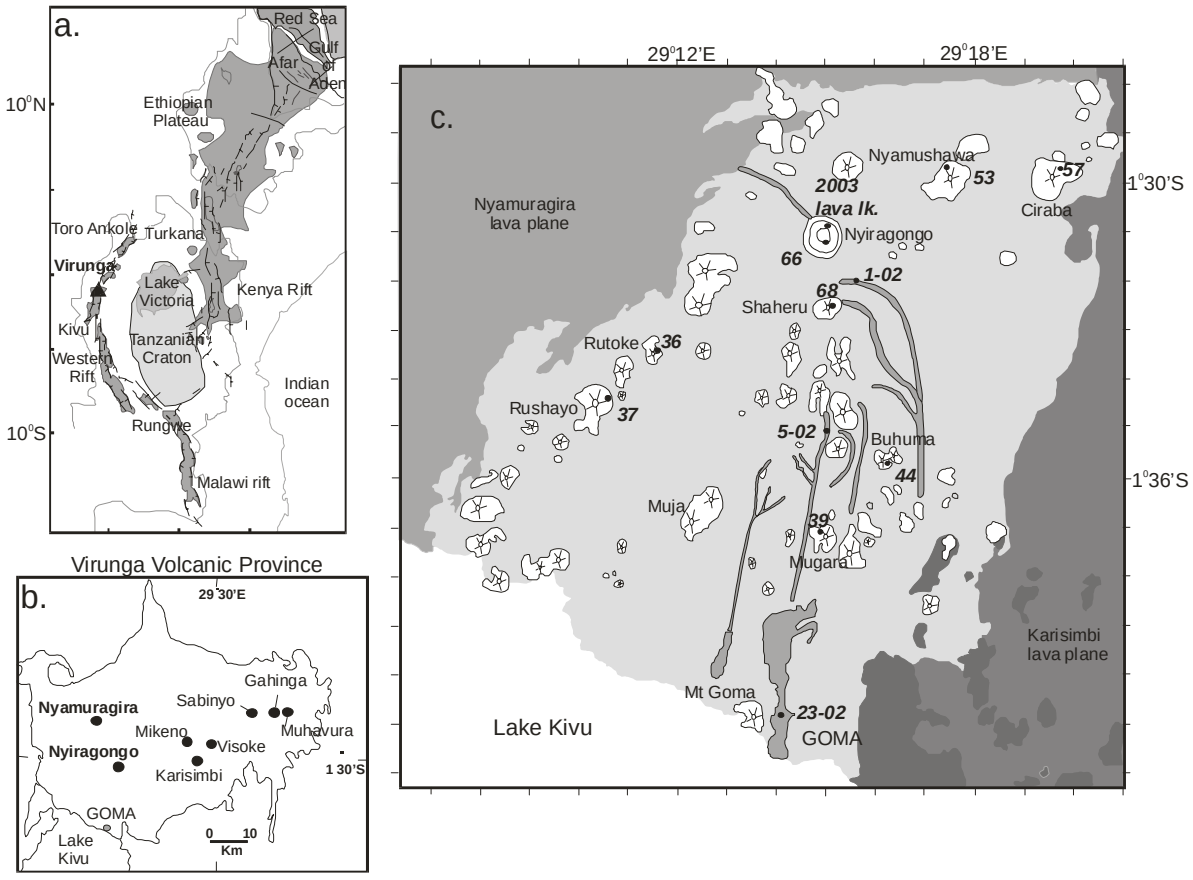

Figure 1. (a) Simplified map showing the major structures of the East African Rift System and location of the Virunga Volcanic Province (VVP) (black triangle). **(b)** Different volcanoes of the VVP including Nyiragongo of the present study. **(c)** Geological map of the Nyiragongo volcanic complex showing several plugs, cones, and the lava plane as well as the locations of the samples of the present study (filled circles, see Table 1). Also shown are the Nyamuragira and Karisimbi volcanic planes.

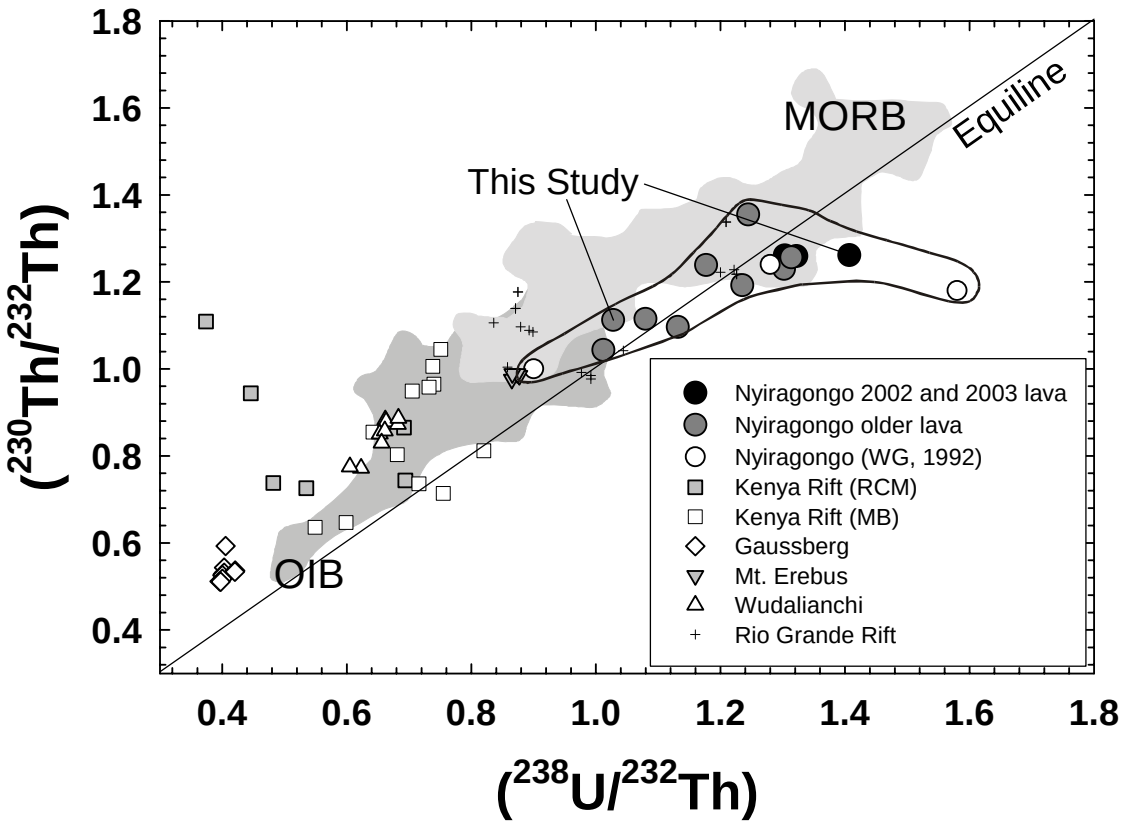

Figure 2. Plot of the activity ratios of $^{230}Th/^{232}Th$ versus $^{238}U/^{232}Th$ (shown in parenthesis) for the Nyiragongo lavas of this study (filled circles, N=13). Our results overlap with previous analyses of the Nyiragongo lavas by Williams and Gill (1992) (open circles) but are strikingly different from those of Tedesco et al. (2007) (not plotted) who reported much higher ($^{238}U/^{232}Th$) ranging from 1.5-2.81. Also shown for comparison are the fields of oceanic basalts (see Sims and Hart, 2006) and continental alkaline volcanics from south-west United States (Asmerom and Edwards, 1995; Asmerom, 1999; Asmerom et al., 2000), Gaussberg (Williams et al., 1992), Mt. Erebus (Sims and Hart, 2006), Wudalianchi (Zou et al., 2003, 2008) and Kenya rift with different basement types (Remobilized cratonic margin or RCM and the late Proterozoic mobile belt or MB) (Rogers et al., 2006). The Nyiragongo lavas plot near to but on both sides of the equiline showing U-Th disequilibria.

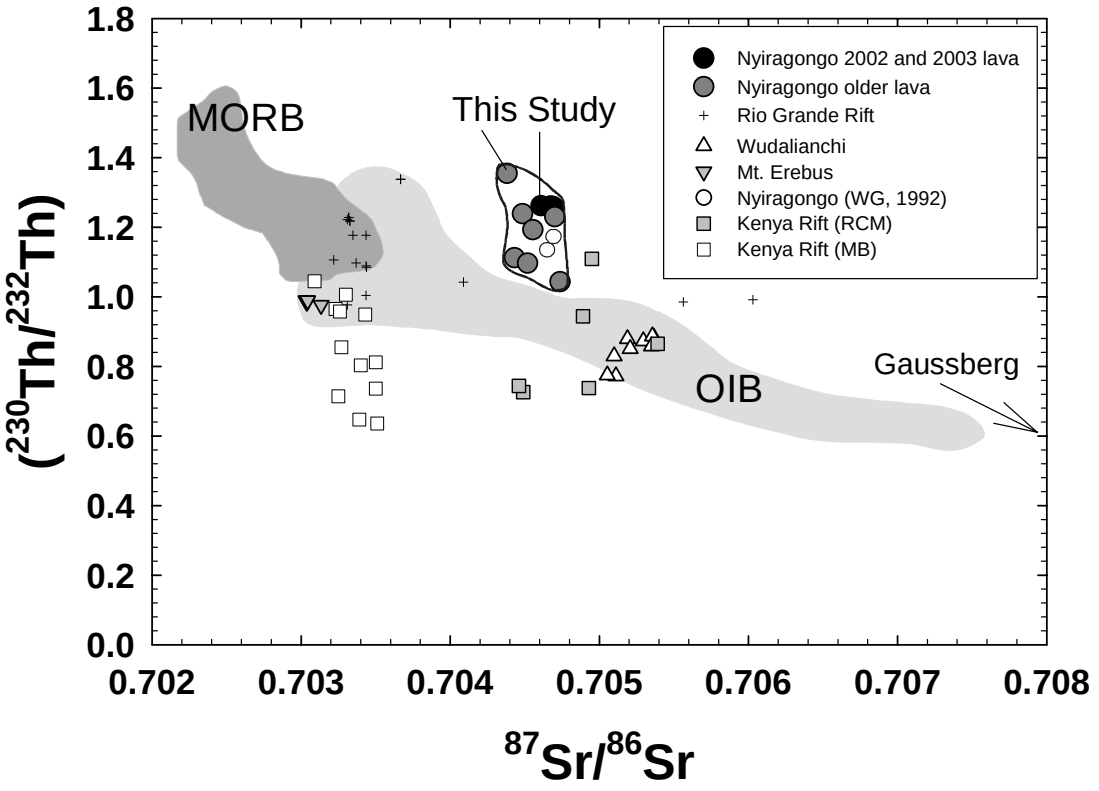

Figure 3. Correlation between (^{230}Th/^{232}Th) and the ^{87}Sr/^{86}Sr. The array defined by oceanic basalts (Sims and Hart, 2006) is shown by the shaded region. Also plotted for comparison are other global continental alkaline volcanics (See Figure 2 caption for details). Nyiragongo lavas of this study (filled circles, N=13) overlap with the analyses of Williams and Gill (1992) (open circles) and lie above this array. The enrichment of ^{230}Th in Nyiragongo relative to other mantle-derived rocks suggests enrichment of the source in ^{238}U and a significant time difference between the metasomatic enrichment and partial melting to allow growth of ^{230}Th.

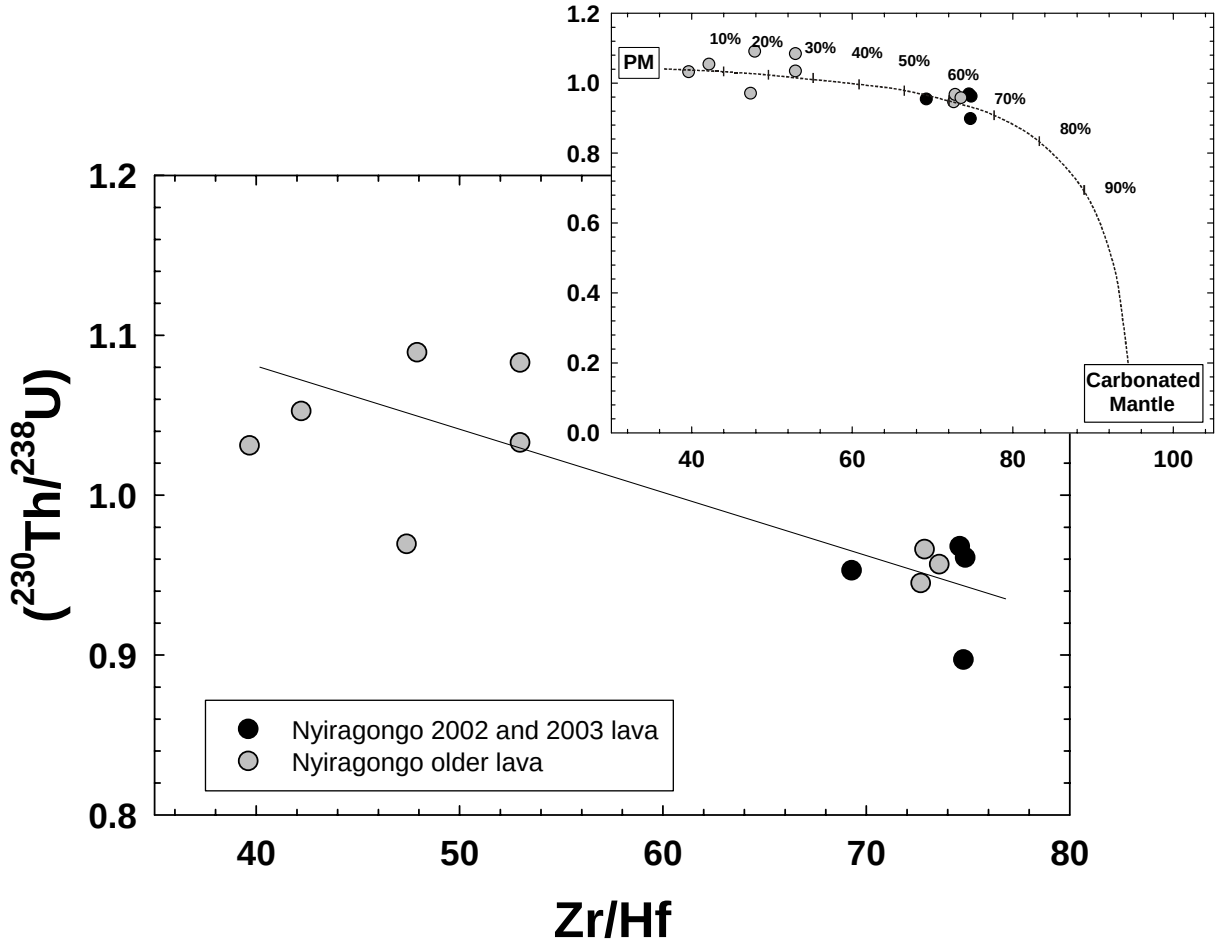

Figure 4. Nyiragongo volcanics of the present study show a rough negative correlation between (^{230}Th/^{238}U) and Zr/Hf, a proxy for carbonate metasomatism, suggesting that carbonate metasomatism in the mantle-source beneath Virunga resulted in ^{238}U excess seen some of these rocks. Our forward modeling results indicate that the youngest Nyiragongo lavas and some historic lava samples were derived from a mantle-source with 50-60% contribution from a carbonatitic end-member while the other historic lavas show up to 20% mixing of a carbonatitic mantle-end member with a primitive mantle end-member. Parameters for the carbonatitic end-member are from Pyle et al. (1991) and some of the parameters for the primitive mantle are from Cambell (2002) and Jochum et al. (1986). Parameters for our best-fit model are as follows: Th/U (carbonatite) = 0.3, Th/U

(primitive mantle) = 4.04, Zr/Hf (Carbonatite) = 100, Zr/Hf (primitive mantle) = 38, (^{230}Th/^{238}U) (carbonatite) = 0.11and (^{230}Th/^{238}U) (primitive mantle) = 1.05

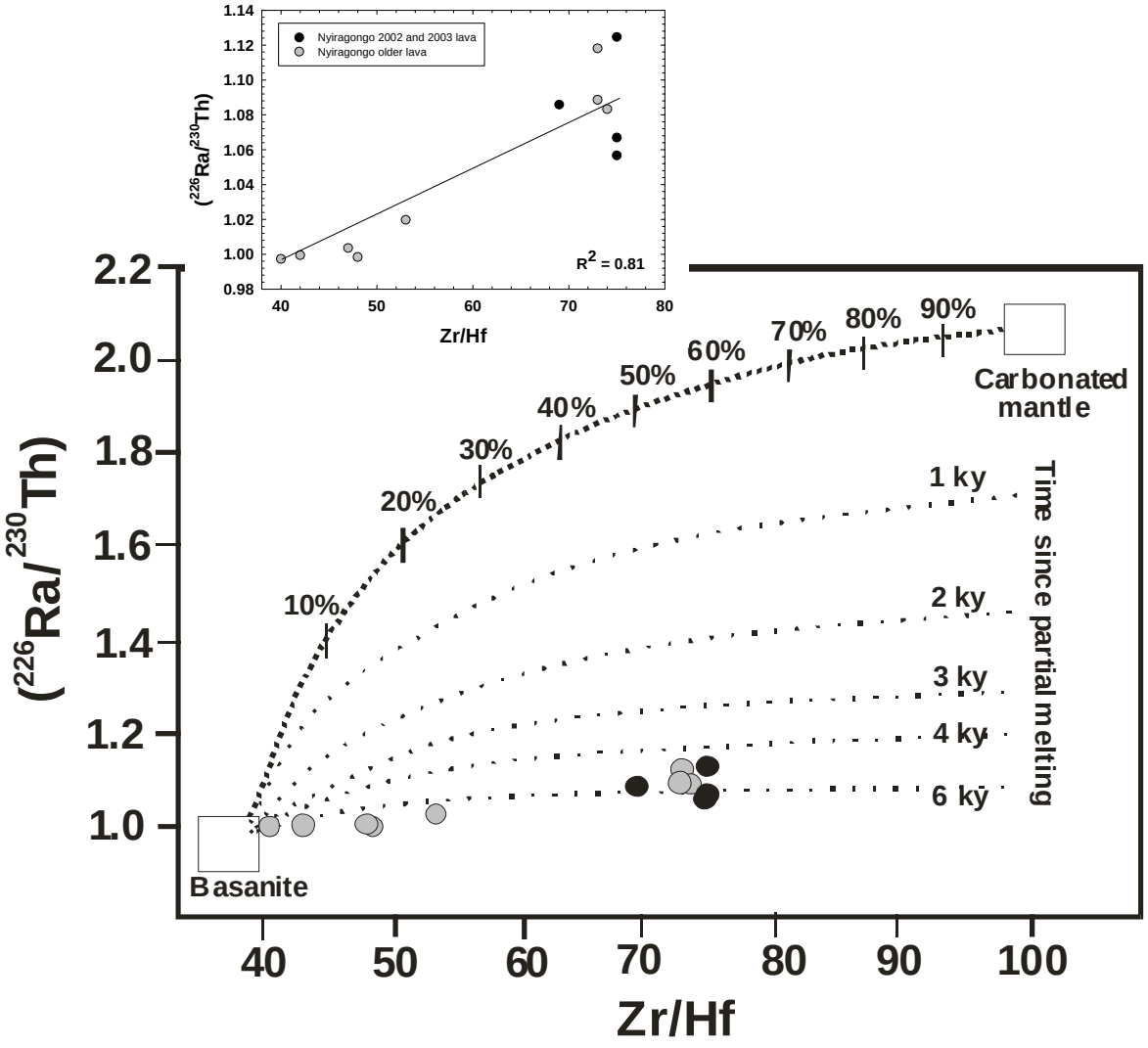

Figure 5. Activity of $^{226}Ra/^{230}Th$ for the Nyiragongo volcanics shows an overall positive correlation with Zr/Hf (inset), a proxy for carbonate metasomatism, suggesting contribution from a carbonate-metasomatized source. Our forward modeling results indicates that younger lavas (black circles) and some of the older unknown-age lava samples (gray circles) show greater contribution (50-60%) from a carbonated mantle component whereas most of the older unknown-age lavas show lesser contribution (2-22%) of this component consistent with our modeling results using ($^{230}Th/^{238}U$) and Zr/Hf as shown in Figure 4.. Our data, however, plot below a simple mixing curve between the above-mentioned end-members. This is an artifact of the time elapsed since partial melting of this mixed source, which produced the Nyiragongo lavas. The lavas with higher Zr/Hf must have erupted within 4-6 ky since partial melting. Parameters for the carbonatitic end-member are from Williams et al. (1986) and

Jochum et al. (1986). Mantle values are from our analyses of basanite lavas from Nyamuragira (Chakrabarti et al., 2009), which will be reported in a different study. Parameters for our best-fit model are as follows: Ra/Th (Carbonatite) = 0.044, Ra/Th (primitive mantle) = 0.008, Zr/Hf (Carbonatite) = 100, Zr/Hf (primitive mantle) = 38, (^{226}Ra/^{230}Th) (carbonatite) = 2.07 and (^{226}Ra/^{230}Th) (primitive mantle) = 1.02.

Timescales of Magmatic Processes and Eruption Ages of the Nyiragongo volcanics from ^{238}U-^{230}Th-^{226}Ra-^{210}Pb disequilibria.

R. Chakrabarti et al.

Appendix 1: Analytical Methods

The protocols for sample preparation and dissolution, ion chromatography, ^{238}U, ^{232}Th and ^{226}Ra concentration and isotope ratio measurements by mass spectrometry as well as gamma spectrometry, as followed in this study, have been described in detail elsewhere (Sims et al., 2008a, b). Here we provide a short summary and present our gamma spectrometry data in Appendix Table 1, which agrees well with our mass spectrometry data as reported in paper.

Almost 12 gm of acid-cleaned 1-5 mm sized rock samples were crushed (<100 μm) using an alumina ball mill. 0.5 gm of each crushed samples was dissolved completely using HF and HNO_3, followed by HNO_3+H_3BO_3 and $HClO_4$ to break down all fluorides. Complete dissolution is critical and was achieved for all samples. The remaining sample powder was used for gamma-counting.

From the dissolved rock samples thorium and uranium were separated and purified in the WHOI clean labs using two anion columns using nitric and hydrochloric acids. Uranium and thorium concentrations on aliquots from the same rock dissolution were determined by isotope dilution using the ThermoFisher Element 2 high resolution sector-field ICPMS at WHOI. Th and U isotopes were measured using the WHOI Thermo Fisher NEPTUNE multi-collector ICPMS. ^{226}Ra concentrations on separate liquid

aliquots from the same rock dissolution were determined by isotope dilution using the Thermo Fisher NEPTUNE at WHOI.

Activities of several short-lived isotopes were measured by gamma spectrometry (Condomines et al., 1987, 1995). Approximately 10 gm of rock powder (grain size < 100 μm) was poured into plastic vials. Each sample vial was inserted into a closed-end coaxial well-type High Purity Germanium (HP-Ge) detector manufactured by CANBERRA that is assembled inside a protective lead and copper shield. The activity of ^{226}Ra was determined using two different gamma rays: 351.99 keV line of ^{214}Pb and the 609.32 keV line of ^{214}Bi. An obsidian standard ATHO from USGS was used to set the efficiency. Estimated errors are for the gamma spectrometry measurements are usually less than 5% (2σ) for (^{226}Ra) based on counting statistics. The accuracy of the gamma spectrometry measurements were indirectly checked by measuring USGS rock standards ATHO and W2 as unknown (Appendix Table 1).

Because the samples are all older than five years, ^{210}Po was measured as a proxy for ^{210}Pb. Analytical techniques for ^{210}Po are discussed in detail elsewhere (Reagan et al., 2005).

Appendix References

Condomines, M. et al., 1987. Short-lived radioactive disequilibria and magma dynamics in Etna volcano. Nature, 325(6105): 607-609.

Condomines, M., Tanguy, J.C. and Michaud, V., 1995. Magma dynamics at Mt. Etna: Constraints from U-Th-Ra-Pb radioactive disequilibria and Sr isotopes in historical lavas. Earth and Planetary Science Letters, 132: 24-41.

Reagan, M.K., Tepley, F.J., Gill, J., Wortel, M. and Hartman, B., 2005. Rapid timescales of basalt to andesite differentiation at Anatahan volcano, Mariana Islands. Journal of Volcanology and Geothermal research, 146: 171-183.

Sims, K.W.W. et al., 2008a. An inter-laboratory assessment of the Th Isotopic Composition of Synthetic and Rock standards. Geostandards and Analytical Research, 32(1): 65-91.

Sims, K.W.W. et al., 2008b. 238U-230Th-226Ra-210Pb-210Po, 232Th-228Ra, and 235U-231Pa constraints on the ages and petrogenesis of Vailulu'u and Malumalu Lavas, Samoa. Geochemistry, Geophysics, Geosystems, 9(4): Q04003,doi:10.1029/2007GC001651.